Chinese Journal of Chemistry
中国化学 - An International Journal

Title: Formation of Functional Cyclooctadiene Derivatives by Supramolecularly-Controlled Topochemical Reactions and Their Use as Highly Selective Fluorescent Biomolecule Probes

Authors: Ming-Ming Gan, and Ying-Feng Han*

This work may now be cited as: *Chin. J. Chem.* **2020**, *38,* 10.1002/cjoc.202000125.

WILEY-VCH SIOC CCS

ISSN 1001-604X • CN 31-1547/O6
mc.manuscriptcentral.com/cjoc
www.cjc.wiley-vch.de

Formation of Functional Cyclooctadiene Derivatives by Supramolecularly-Controlled Topochemical Reactions and Their Use as Highly Selective Fluorescent Biomolecule Probes

Ming-Ming Gan,[a] and Ying-Feng Han*,[a,b]

[a]Key Laboratory of Synthetic and Natural Functional Molecule Chemistry, College of Chemistry and Materials Science, Northwest University, Xi'an 710127, P. R. China
[b]State Key Laboratory of Structural Chemistry, Fujian Institute of Research on the Structure of Matter, Chinese Academy of Sciences, Fuzhou, Fujian 350002, P. R. China

Cite this paper: *Chin. J. Chem.* **2019**, *37*, XXX—XXX. **DOI: 10.1002/cjoc.201900XXX**

Summary of main observation and conclusion Controlling the regio- and stereochemistry of the photoproducts in solution is far more challenging for polyenes than for monoalkenes. Herein, a supramolecularly-controlled topochemical reaction of conjugated dienes in homogeneous system is developed, ultimately providing two cyclooctadiene-cored tetraimidazolium molecular receptors exclusively. These cyclooctadiene derivatives exhibited highly sensitive and selective fluorescence sensing for thymine relative to other biologically relevant species in aqueous solution at physiological pH. Both the cyclooctadiene moieties and imidazolium units play important roles in the selective recognition observed. The presented supramolecularly-controlled method allows the simple yet rare selective photoconversion of flexible cyclooctadiene derivatives in solution. This study offers a new synthetic strategy for the preparation of functional molecules with potential for use in biological applications.

Background and Originality Content

Template-controlled supramolecular synthesis (e.g. those using coordination bonds, hydrogen bonds, halogen bonds, cation···π, π···π, and halogen···halogen interactions) has been found to be a useful method to align pairs of C=C bonds to meet Schmidt's postulate and allow photochemical reactions to proceed. However, most of these photoreactions were limited to the solid or crystalline states.[1-3] The control of the regio- and stereoselectivity of photo-induced transformations in homogeneous solutions remains a significant challenge, with limitations related to the solubility of the supramolecular assemblies, maintaining the appropriate orientation of the conjugated C=C bonds and the formation of mixtures of compounds due to *cis*-*trans*-isomerization.[4]

The scope of the substrates used in photochemical reactions of this type is largely limited to monoalkenes, as polyenes have multiple reactive sites, opening the possibility of [2+2] or [4+4] cycloaddition reactions or other reactions, and thus the potential formation of a number of regio- and stereoisomers, *E*/*Z* isomers, and even polymers (Scheme 1).[5-7] Therefore, controlling the regio- and stereochemistry of the photoproducts is far more challenging for polyenes than for monoalkenes.[8,9] Recently, we developed a strategy for the preparation of a series of polyimidazolium cyclobutane derivatives by applying metal-carbene template-directed [2+2] cycloaddition reactions in homogeneous solution.[10,11] We expected this method to be applicable for the construction of functional molecules of increasing structural complexity; our goal was not only to utilize this metal-carbene-templated photochemical reaction to generate new complexes but also to produce functional receptors for biomolecular sensing.

Due to their effective binding with guest species through ionic $(C\text{-}H)^{+}\cdots A^{-}$ hydrogen-bonding interactions, fluorescent imidazolium-based receptors have been extensively investigated in recent years due to their simplicity and the high sensitivity afforded by changes in their fluorescence intensity.[12] The scope of application of imidazolium-based receptors in sensing is often limited to small anions, with the exception of a few examples describing the sensing of biomolecules.[13,14] Indeed, it is still challenging to design scaffolds for the specific recognition of biologically relevant targets, especially host molecules that are soluble in aqueous solution at physiological pH. Herein, we demonstrate a supramolecularly-controlled topochemical photoreaction in solution that provides two cyclooctadiene-cored tetraimidazolium receptor molecules. Due to their flexible

Scheme 1 Possible photoproducts obtained by the photoreaction of symmetrical diene

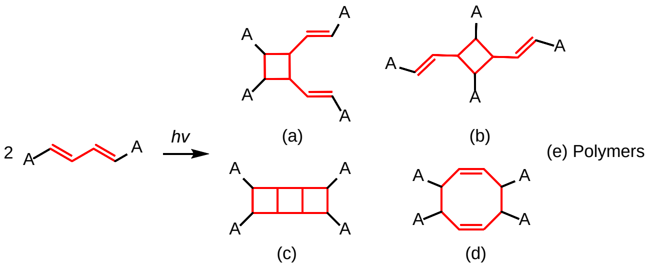

cyclooctadiene moieties and imidazolium-based receptor sites, the cyclooctadiene derivatives exhibit highly sensitive and selective fluorescence sensing for thymine relative to other relevant molecules in aqueous solution at physiological pH (7.4). The key step in the synthesis of the receptor is the formation of a cyclooctadiene ring by a photo-induced topochemical reaction facilitated by supramolecular templates. A series of dinuclear Ag^{I} and Au^{I} molecular rectangles featuring dienyl-bridged dicarbene ligands were designed and synthesized, wherein the preorganization of the pairs of dienyl units brings them into close enough proximity to allow further photochemical modification (Scheme 2). Facile removal of the metal ions by cleavage of the metal-carbene bond then affords cyclooctadiene-cored tetraimidazolium compounds. This supramolecularly-controlled method allows the simple yet rare selective photoconversion of flexible cyclooctadiene derivatives in solution.

Scheme 2 Preparation and reactions of dicarbene-derived metallacycles to afford cyclooctadienes

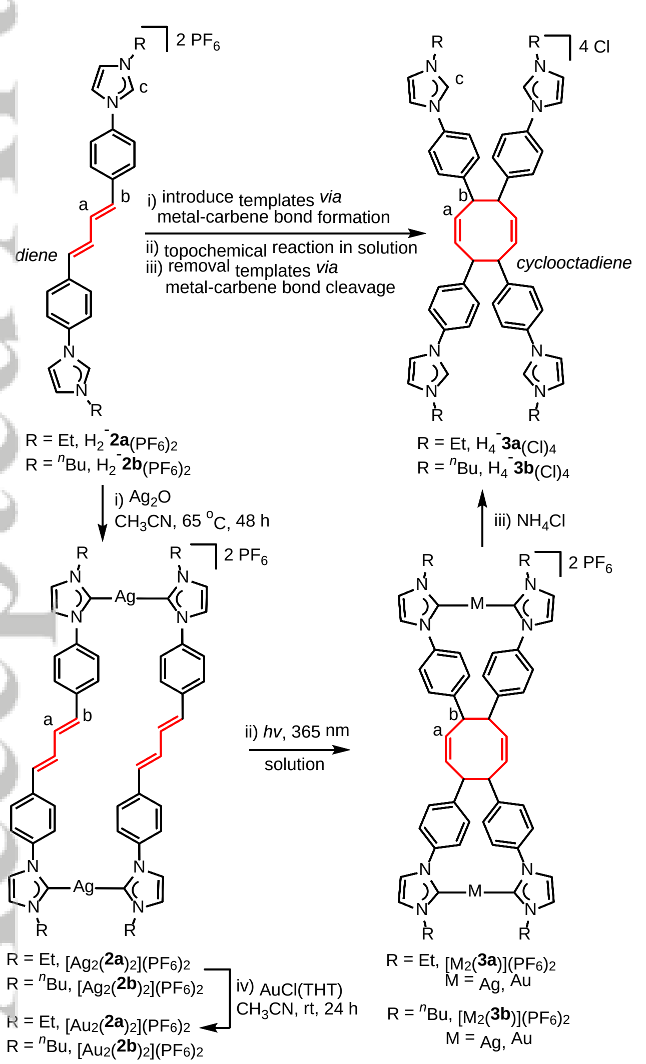

Results and Discussion

Bis(imidazolium)-substituted diene derivatives H_2-**L**$(PF_6)_2$ (**L** = **2a**, **2b**) were prepared from (1*E*, 3*E*)-1,4-bis(4-(1H-imidazol-1-yl)phenyl)buta-1,3-diene (**1**)[15] using a similar reported procedure (see Supporting Information (SI), Scheme S1).[11d] The *1E,3E* structure of the proligand was confirmed by X-ray diffraction analysis of crystals of H_2-**L**$(PF_6)_2$ (Figure 1). As shown in Scheme 2, the dinuclear tetracarbene complexes $[Ag_2(\mathbf{L})_2](PF_6)_2$ (**L** = **2a**, **2b**) were synthesized in excellent yields by the reaction of bisimidazolium salts H_2-**L**$(PF_6)_2$ (**L** = **2a**, **2b**) with excess Ag_2O in acetonitrile at 65 °C for 48 h under the exclusion of light (see SI).

In contrast to the proligands H_2-**L**$(PF_6)_2$, the characteristic resonances of the C2-H protons of the imidazolium salts were not observed in the ^1H NMR spectra of silver(I) carbene complexes $[Ag_2(\mathbf{L})_2](PF_6)_2$ (**L** = **2a**, **2b**) (Figure 2a,c and S1). In the $^{13}C\{^1H\}$ NMR spectra of the complexes, characteristic C_{NHC} resonances for $[Ag_2(\mathbf{2a})_2](PF_6)_2$ and $[Ag_2(\mathbf{2b})_2](PF_6)_2$ were observed at δ = 178.1 and 178.3 ppm, respectively, which are typical values for silver(I) carbene complexes. The electrospray ionization mass spectra (ESI-MS) in positive mode further supported the formation of the silver(I) complexes. For example, the ESI-MS spectra showed peaks at m/z = 502.1441 (calcd for $[Ag_2(\mathbf{2a})_2]^{2+}$ 502.1204) and m/z = 558.1842 (calcd for $[Ag_2(\mathbf{2b})_2]^{2+}$ 558.1831) (see SI).

Gold(I) carbene complexes $[Au_2(\mathbf{L})_2](PF_6)_2$ (**L** = **2a**, **2b**) were synthesized by treating the corresponding silver(I) carbene complexes $[Ag_2(\mathbf{L})_2](PF_6)_2$ with 2 equiv of [AuCl(THT)] (THT = tetrahydrothiophene) in acetonitrile at ambient temperature for 24 h under exclusion of light (Scheme 2). These gold(I) complexes were isolated as air- and moisture-stable off-white solids in yields of 82% and 79%, respectively. Both complexes were fully characterized by NMR spectroscopy and ESI-MS analysis (see SI). The structure of $[Au_2(\mathbf{2a})_2](PF_6)_2$ was further confirmed by X-ray diffraction (Figure 3). The gold(I) atoms are coordinated to the NHC ligands in a linear fashion with C_{NHC}–Au–C_{NHC} angles of 173.7 and 176.2°, and Au–C_{NHC} distances between 1.996 and 2.042 Å. The Au–NHC bonds of this gold(I) complex bring the diene moieties into closely proximity in a "face-to-face" manner with distances between the pairs of olefin C=C bonds of ca. 4.2 Å.

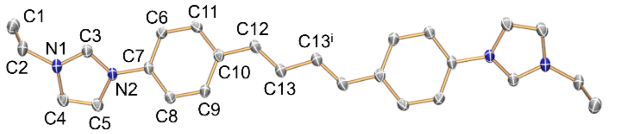

Figure 1 ORTEP view of ligand H_2-**2a**$(PF_6)_2$ with 50% ellipsoid probability and hydrogen atoms omitted for clarity. Selected bond lengths (Å) and angles (deg): N(1)–C(3) 1.326(2), N(2)–C(3) 1.336(2), C(10)–C(12) 1.463(2), C(12)–C(13) 1.337(2), C(13)–C(13$^{\#}$) 1.447(3); N(1)–C(3)–N(2) 108.44(13), C(13)–C(12)–(C10) 126.90(15).

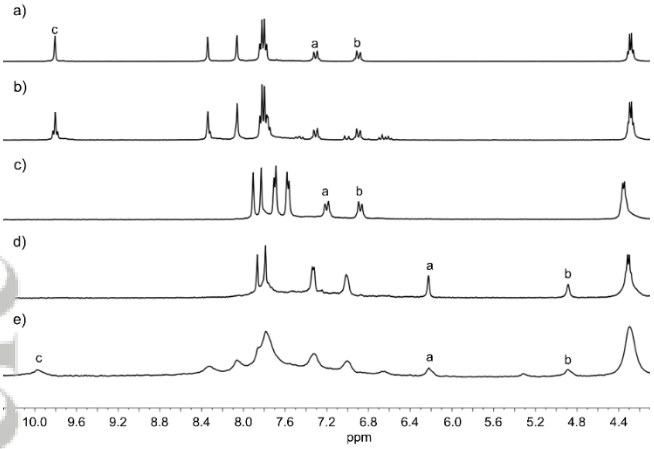

Figure 2 ^{1}H NMR spectra (400 MHz, 298 K, [D$_6$]DMSO) of complexes. Partial ^{1}H NMR spectra of H$_2$-**2a**(PF$_6$)$_2$ (a) before and (b) after UV irradiation; of [Ag$_2$(**2a**)$_2$](PF$_6$)$_2$ (c) before and (d) after irradiation; and of (e) H$_4$-**3a**(Cl)$_4$.

Photoreaction of [M$_2$(**L**)$_2$](PF$_6$)$_2$ (M = Ag, Au; **L** = **2a**, **2b**) in [D$_6$]DMSO at ambient temperature with a Xe lamp (λ = 365 nm) revealed the clear formation of corresponding cyclooctadiene-carbene complexes [M$_2$(**L**)](PF$_6$)$_2$ (M = Ag, Au; **L** = **3a**, **3b**) in nearly quantitative conversion, respectively (Figure 2, S1-3). All complexes were well characterized by multinuclear NMR spectroscopy and ESI-MS spectrometry. In a typical experiment, the formation of cyclooctadiene-carbene complexes can be reliably monitored by ^{1}H NMR spectroscopy. For example, doublet resonances for the diene protons of H$_a$ and H$_b$ in [Ag$_2$(**2a**)$_2$](PF$_6$)$_2$, at δ = 7.20 and 6.88 ppm, are not observed in [Ag$_2$(**3a**)](PF$_6$)$_2$ after irradiation. Instead, a new characteristic pair of relatively high-field proton signals at δ = 6.23 and 4.88 ppm in a 1:1 intensity ratio confirmed the assignment of the cyclooctadiene-containing structure of the silver(I) carbene complexes (Figure 2c,d). The ^{13}C{^{1}H} NMR spectrum of [Ag$_2$(**3a**)](PF$_6$)$_2$ further verified the formation of the cyclooctadiene ring with characteristic resonances at δ = 131.3 and 49.5 ppm. To investigate this irradiation progress further, we collected aliquots of the mixture of [Ag$_2$(**2a**)$_2$](PF$_6$)$_2$ under UV irradiation at various time intervals and acquired their ^{1}H NMR spectra, (Figure S4) which indicated the gradual disappearance of the diene resonances and appearance of two new peaks for the cyclooctadiene ring (but no other new signals corresponding to intermediate [2+2] cyclobutane products) and that the photoreaction was completed in 80 mins. In addition, the conversions were also monitored by UV-vis, fluorescence and IR experiments (Figure S5-9).[16]

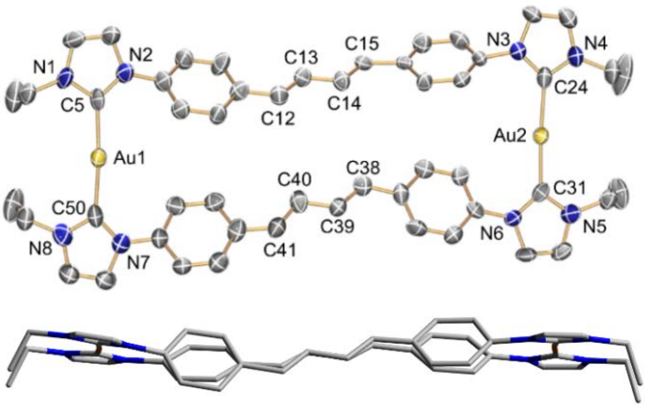

Figure 3 X-ray structure of [Au$_2$(**2a**)$_2$](PF$_6$)$_2$ (top) ORTEP view with 50% ellipsoid probability and (bottom) side view. Anions and hydrogen atoms omitted for clarity. Selected bond lengths (Å) and angles (deg): C13−C12 1.337(15), C14−C13 1.433(15), C15−C14 1.330(15), C38−C39 1.332(16), C40−C39 1.452(16), C41−C40 1.318(17), Au1−C5 2.020(12), Au1−C50 2.025(13), Au2−C24 2.042(12), Au2−C31 1.996(11); C5−Au1−C50 173.7(5), C31−Au2−C24 176.2(4).

Testing this reaction in the absence of the metal-carbene template, no [4+4] or [2+2] cycloaddition products were formed by treating the proligand H$_2$-**2a**(PF$_6$)$_2$ under the same conditions, even with extension of the irradiation time to 8 h (Figure 2b). These results demonstrate that two pairs of conjugated olefins possess comparable photochemical reactivity and that the exclusive formation of the cyclooctadiene product is obviously controlled by steric restriction upon metal-carbene rigidification within the metallarectangle architecture. The cyclooctadiene tetraimidazolium salts H$_4$-**L**(Cl)$_4$ (**L** = **3a**, **3b**) were subsequently isolated by the removal of the silver cations by treatment with NH$_4$Cl in methanol and removal of the precipitated AgCl. The ^{1}H NMR spectrum of H$_4$-**3a**(Cl)$_4$ showed broad peaks that can be explained by the flexibility of the cyclooctadiene rings and the inequivalent protons of the phenylene rings and imidazolium units (Figure 2e). The ESI-MS data provided further evidence for the formation of the desired tetraimidazolium salts.

A biomolecule recognition experiment was conducted by measuring the fluorescence variation of the imidazolium salt

H_4-**3a**(Cl)$_4$ (30 μM) upon addition of 20 equiv of a variety of biomolecules under physiological conditions (10 mM phosphate buffer at pH = 7.4) at λ_{ex} = 282 nm. As shown in Figure 4, the fluorescence of H_4-**3a**(Cl)$_4$ was significantly quenched upon the addition of thymine (T). In contrast, only minor changes were observed upon addition of 20 equiv of a series of amino acids, such as homocysteine (Hcy), alanine (Ala), proline (Pro), threonine (Thr), glycine (Gly), leucine (Leu), isoleucine (Ile), valine (Val), serine (Ser), asparagine (Asn), phenylalanine (Phe), penicillamine (Pen), cysteine (Cys), methionine (Met), arginine (Arg) and histidine (His). No obvious change was observed upon addition of excess glutathione (GSH), fructose (Fru) or glucose (Glc) (Figure 4c). Furthermore, only minor changes were observed upon addition of 20 equiv of different inorganic anion species, including F^-, Cl^-, Br^-, I^-, CO_3^{2-}, HCO_3^-, HSO_3^-, SO_3^{2-}, $S_2O_3^{2-}$, NO_3^-, NO_2^-,

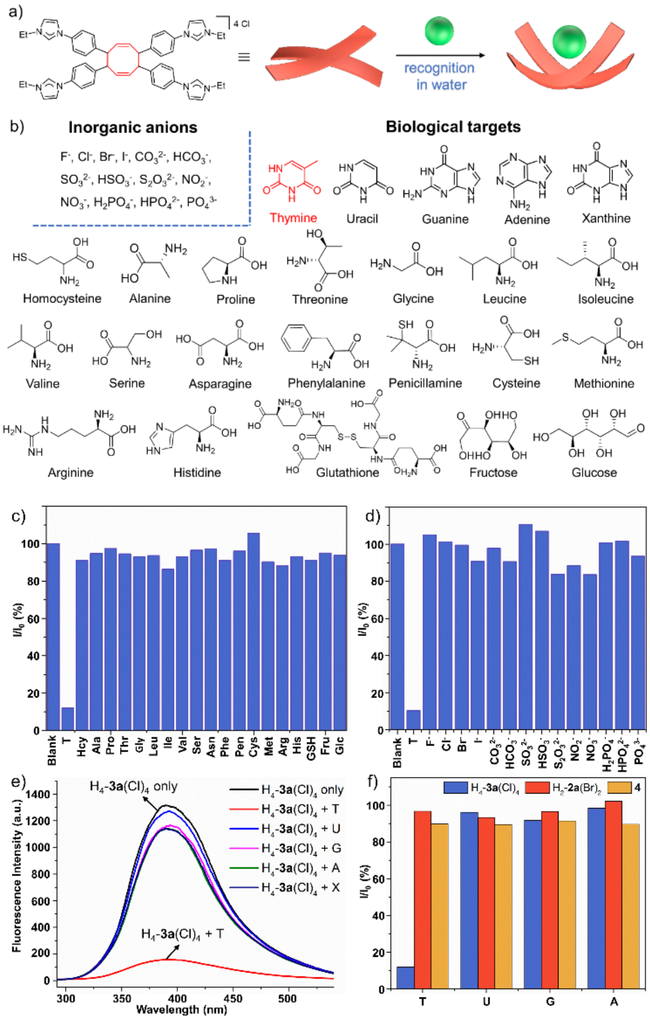

Figure 4 Fluorescence responses of hosts to biomolecules. (a) Schematic representation of the binding interaction between H_4-**3a**(Cl)$_4$ and biological species. (b) The inorganic anions and biomolecules in this study. (c) Fluorescence responses of H_4-**3a**(Cl)$_4$ (30 μM) to various biomolecules at pH = 7.4 (10 mM phosphate buffer) (excitation at 282 nm). The bars represent the fluorescence responses (λ_{em} = 390 nm) upon addition of 20 equiv of the respective biomolecule. (d) Fluorescence responses of H_4-**3a**(Cl)$_4$ (30 μM) at λ_{em} = 390 nm with 20 equiv of the respective anion species. (e) Fluorescent emission changes of H_4-**3a**(Cl)$_4$ (30 μM) upon addition of T, U, G, A, and X (20 equiv) at pH = 7.4 (10 mM phosphate buffer). (d) Fluorescence responses of different hosts (30 μM) to biomolecules at pH = 7.4. I and I_0 was the fluorescence intensity of the H_4-**3a**(Cl)$_4$ only and the H_4-**3a**(Cl)$_4$ after guest added.

$H_2PO_4^-$, HPO_4^{2-}, PO_4^{3-} (Figure 4d).

To further evaluate whether H_4-**3a**(Cl)$_4$ exhibits high selectivity for thymine, the fluorescence changes were measured upon addition of the structurally similar biomolecules including uracil (U), guanine (G), adenine (A), xanthine (X). Surprisingly, each of these species induced almost negligible changes compared to that caused by thymine (Figure 4e). Competitive binding experiments were also conducted in the presence of different inorganic anions and uracil (U) at 20 equiv, respectively, with the subsequent addition of 20 equiv of thymine (Figure S10,11). No significant variation in the fluorescence intensity was observed except for with thymine.

To our surprise, no selectivity for thymine over other biomolecules was observed when bisimidazolium salt H_2-**2a**(Br)$_2$ or cyclobutane-based tetraimidazolium salt (**4**) were used as receptor under the above conditions (Figure 4f, S12). These results imply that both the cyclooctadiene and imidazolium units play important roles in the selective recognition for thymine, however, the binding mode in solution needs to be confirmed by further detailed investigations.

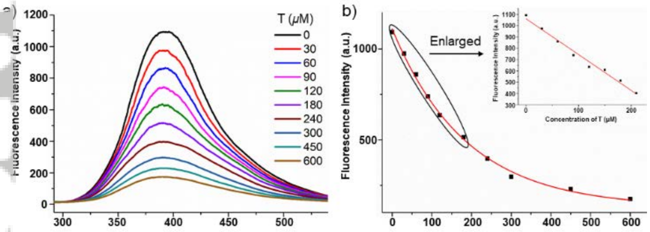

Figure 5 The behavior of H_4-**3a**(Cl)$_4$ and thymine. (a) Fluorescence spectra of H_4-**3a**(Cl)$_4$ (30 μM) in the presence of increasing concentrations of thymine at pH = 7.4 (10 mM phosphate buffer) (excitation at 282 nm). (b) The fluorescence intensity at 390 nm as function of thymine concentration.

In order to gain a detailed understanding of the detection behavior of H_4-**3a**(Cl)$_4$ and thymine, a fluorescence titration of thymine was undertaken (Figure 5a). The result clearly shows the fluorescence quenching effect at 390 nm with increasing concentration of thymine (1−20 equiv). Furthermore, a plot of fluorescence intensities of H_4-**3a**(Cl)$_4$ versus thymine concentration at λ_{em} = 390 nm was prepared. The plots of thymine illustrated a good linear relationship between intensity and thymine concentration (Figure 5b). The binding ratio of the host-guest complex was determined by a Job's plot analysis and found to be 1:1 (Figure S13). The association constant (K_a) was calculated by Benesi-Hilderbrand apparatus and found to be 4.07 × 10^3 M^{-1} (Figure S14).

Conclusions

In conclusion, we have successfully synthesized the cyclooctadiene tetraimidazolium compounds H_4-**L**(Cl)$_4$ (**L** = **3a**, **3b**) in a rapid and quantitative conversion though a metal-carbene-templated photochemical [4+4] cycloaddition in solution. Moreover, the cyclooctadiene imidazolium derivatives can be applied as fluorescent chemosensors that sense thymine selectively through fluorescence quenching over other biologically relevant biomolecules in aqueous solution of physiological pH (7.4). In the future, we hope to realize the application of this type of photoproducts for detecting biologically relevant targets (such as nucleic acids), which would mark a significant achievement in the field of host-guest systems. We anticipate that the present method could serve as a new tool in the synthesis of unique functional molecules with potential applications in biological studies.

Supporting Information

The supporting information for this article is available on the WWW under https://doi.org/10.1002/cjoc.2019xxxxx. CCDC 1976920 and 1976922 contain the supplementary crystallographic data for this paper. These data are provided free of charge by The Cambridge Crystallographic Data Centre.

Acknowledgement

The authors gratefully acknowledge financial support from the National Natural Science Foundation of China for Outstanding Youth Scholars (grant nos. 21722105), the National Youth Top-notch Talent Support Program of China, the Key Science and Technology Innovation Team of Shaanxi Province (2019TD-007, 2019JLZ-02), and the FM&EM International Joint Laboratory of Northwest University.

References

[1] (a) Ramamurthy, V.; Sivaguru, J. Supramolecular Photochemistry as a Potential Synthetic Tool: Photocycloaddition. *Chem. Rev.* **2016**, *116*, 9914−9993; (b) Biradha, K.; Santra, R. Crystal Engineering of Topochemical Solid State Reactions. *Chem. Soc. Rev.* **2013**, *42*, 950−967; (c) Gan, M.-M.; Yu, J.-G.; Wang, Y.-Y.; Han, Y.-F. Template-Directed Photochemical [2+2] Cycloaddition in Crystalline Materials: A Useful Tool to Access Cyclobutane Derivatives. *Cryst. Growth Des.* **2018**, *18*, 553−565; (d) Gan, M.-M.; Zhang, W.; Huo, X.-K.; Han, Y.-F. Template-Directed Photochemical [2+2] Cycloaddition within Discrete Assemblies. *Sci. Sin. Chim.* **2017**, *47*, 705−712 (in Chinese).

[2] (a) Rupasinghe, T. P.; Hutchins, K. M.; Bandaranayake, B. S.; Ghorai, S.; Karunatilake, C.; Bučar, D.-K.; Swenson, D. C.; Arnold, M. A.; MacGillivray, L. R.; Tivanski, A. V. Mechanical Properties of a Series of Macro- and Nanodimensional Organic Cocrystals Correlate with Atomic Polarizability. *J. Am. Chem. Soc.* **2015**, *137*, 12768−12771; (b) Du, J.; Skubi, K. L.; Schultz, D. M.; Yoon, T. P. A Dual-Catalysis Approach to Enantioselective [2+2] Photocycloadditions using Visible Light. *Science* **2014**, *344*, 392−396; (c) Shi, Y.-X.; Zhang, W.-H.; Abrahams, B. F.; Braunstein, P.; Lang, J.-P. Fabrication of Photoactuators: Macroscopic Photomechanical Responses of Metal–Organic Frameworks to Irradiation by UV Light. *Angew. Chem. Int. Ed.* **2019**, *58*, 9453–9458; (d) Maddipatla, M. V. S. N.; Pattabiraman, M.; Natarajan, A.; Srivastav, K.; Mague, J. T.; Ramamurthy, V. Regioselective Photodimerization of Pyridyl-Butadienes within

Cucurbit[8]uril Cavities. *Org*. *Biomol*. *Chem*. **2012**, *10*, 9219–9222; (e) Hu, F.-L.; Mi, Y.; Zhu, C.; Abrahams, B. F.; Braunstein, P.; Lang, J.-P. Stereoselective Solid-State Synthesis of Substituted Cyclobutanes Assisted by Pseudorotaxane-Like MOFs. *Angew*. *Chem*. *Int*. *Ed*. **2018**, *57*, 12696–12701.

[3] (a) Tang, X.; Huang, Z.; Chen, H.; Kang, Y.; Xu, J.-F.; Zhang, X. Supramolecularly Catalyzed Polymerization: From Consecutive Dimerization to Polymerization. *Angew*. *Chem*. *Int*. *Ed*. **2018**, *57*, 8545–8549; (b) Oburn, S. A.; Swenson, D. C.; Mariappan, S. V. S.; MacGillivray, L. R. Supramolecular Construction of an Aldehyde−Cyclobutane via the Solid State: Combining Reversible Imine Formation and Metal−Organic Self-Assembly. *J*. *Am*. *Chem*. *Soc*. **2017**, *139*, 8452−8454; (c) Campillo-Alvarado, G.; D'mello, K. P.; Swenson, D. C.; Mariappan, S. V. S.; Höpfl, H.; Morales-Rojas, H.; MacGillivary, L. R. Exploiting Boron Coordination: B←N Bond Supports a [2+2] Photodimerization in the Solid State and Generation of a Diboron Bis-Tweezer for Benzene/Thiophene Separation. *Angew*. *Chem*. *Int*. *Ed*. **2019**, *58*, 5413–5416; (d) Wang, L.-F.; Zhuang, W.-M.; Huang, G.-Z.; Chen, Y.-C.; Qiu, J.-Z.; Ni, Z.-P.; Tong, M.-L. Spin-Crossover Modulation via Single-Crystal to Single-Crystal Photochemical [2+2] Reaction in Hofmann-Type Frameworks. *Chem*. *Sci*. **2019**, *10*, 7496–7502; (e) Guo, J.; Fan, Y.-Z.; Lu, Y.-L.; Zheng, S.-P.; Su, C.-Y. Visible-Light Photocatalysis of Asymmetric [2+2] Cycloaddition in Cage-Confined Nanospace Merging Chirality with Triplet-State Photosensitization. *Angew*. *Chem*. *Int*. *Ed*. **2020**, https://doi.org/10.1002/anie.201916722.

[4] (a) Bibal, B.; Mongin, C.; Bassani, D. M. Template Effects and Supramolecular Control of Photoreactions in Solution. *Chem*. *Soc*. *Rev*. **2014**, *43*, 4179–4198; (b) Cao, C.; Lang, J.-P. Metal-Carbene Unit: A Universal Tool towards High-Efficient Photochemical Reaction in Solution. *Sci. China Chem.* **2019**, 62, 655–656; (c) Qin, Y.; Zhang, Y.; Yin, G.; Wang, Y.; Zhang, C.; Chen, L.; Tan, H.; Li, X.; Xu, L.; Yang, H. Construction of Highly Emissive Pt(II) Metallacycles upon Irradiation. *Chin. J. Chem.* **2019**, *37*, 323–329.

5] Yu, J.-G.; Gan, M.-M.; Bai, S.; Han, Y.-F. Photodriven Solid-State Multiple [2+2] Cycloaddition Strategies for the Construction of Polycyclobutane Derivatives. *CrystEngComm* **2019**, *21*, 4673–4683.

[6] (a) Lahav, M.; Schmidt, G. M. J. Topochemistry. part XXIII. The Solid-State Photochemistry at 25° of Some Muconic Acid Derivatives. *J*. *Chem*. *Soc*. *B* **1967**, 312−317; (b) Kole, G. K.; Chanthapally, A.; Tan, . K.; Vittal, J. J. Solid State Packing and Photoreactivity of Alkali Metal Salts of *trans*,*trans*-Muconate. *Cryst*. *Growth Des*. **2015**, *15*, 5555−5559; (c) Gao, X.; Friščić, T.; MacGillivray, L. R. Supramolecular Construction of Molecular Ladders in the Solid State. *Angew*. *Chem*. *Int*. *Ed*. **2004**, *43*, 232–236; (d) Mir, M. H.; Ong, J. X.; Kole, G. K.; Tan, G. K.; McGlinchey, M. J.; Wu, Y.; Vittal, J. J. Photoreactive Gold(I) Macrocycles with Diphosphine and *trans*,*trans*-Muconate Ligands. *Chem*. *Commun*. **2011**, *47*, 11633–11635; (e) Wang, Z.; Miller, B.; Butz, J.; Randazzo, K.; Wang, Z. D.; Chu, Q. R. Polyladderane Constructed from a Gemini Monomer through Photoreaction. *Angew*. *Chem*. *Int*. *Ed*. **2017**, *56*, 12155–12159.

7] (a) Meng, F.; Min, J.; Wang, C.; Wang, L. Preparation of Cocrystals of 1,4-Diimidazolylbutadiene with a Template Molecule and Dependence of the Cocrystal Photochemical Products on Wavelength. *Eur. J. Org. Chem.* **2016**, 2220−2225; (b) Park, I.-H.; Medishetty, R.; Lee, H.-H.; Mulijanto, C. E.; Quah, H. S.; Lee, S. S.; Vittal, J. J. Formation of a Syndiotactic Organic Polymer Inside a MOF by a [2+2] Photo-Polymerization Reaction. *Angew*. *Chem*. *Int*. *Ed*. **2015**, *54*, 7313−7317; (c) Balgley, R.; de Ruiter, G.; Evmenenko, G.; Bendikov, T.; Lahav, M.; van der Boom, M. E. Light-Induced Conversion of Chemical Permeability to Enhance Electron and Molecular Transfer in Nanoscale Assemblies. *J*. *Am*. *Chem*. *Soc*. **2016**, *138*, 16398−16406; (d) Guo, L.; Yang, X.; Cong, H. Synthesis of Macrocyclic Oligoparaphenylenes Derived from Anthracene Photodimer. *Chin. J. Chem.* **2018**, *36*, 1135–1138; (e) Chen, X.-M.; Chen, Y.; Liu, Y. Multiple-Stimuli Responsive and Tunable Luminescent Supramolecular Assembly by Oligo(*p*-phenylvinylene) and Surfactant. *Chin. J. Chem.* **2018**, *36*, 526–530; (f) Park, I.; Lee, E.; Lee, S. S.; Vittal, J. J. Chemical Patterning in Single Crystals of Metal–Organic Frameworks by [2+2] Cycloaddition Reaction. *Angew*. *Chem*. *Int*. *Ed*. **2019**, *58*, 14860–14864; (g) Mandal, R.; Garai, A.; Peli, S.; Datta, P. K.; Biradha, K. Photoinduced Bending of Single Crystals of a Linear Bis-Olefin via Water-Templated Solid-State [2+2] Photopolymerization Reaction. *Chem*. *Eur*. *J*. **2020**, *26*, 396–400.

[8] (a) Paradies, J.; Greger, I.; Kehr, G.; Erker, G.; Bergander, K.; Fröhlich, R. Formation of an Organometallic Ladderane Derivative by Dynamic Topochemical Reaction Control. *Angew*. *Chem*. *Int*. *Ed*. **2006**, *45*, 7630–7633; (b) Gong, W.-J.; Ren, Z.-G.; Li, H.-X.; Zhang, J.-G.; Lang, J.-P. Cadmium(II) Coordination Polymers of 4-Pyr-Poly-2-Ene and Carboxylates: Construction, Structure, and Photochemical Double [2+2] Cycloaddition and Luminescent Sensing of Nitroaromatics and Mercury(II) Ions. *Cryst*. *Growth Des*. **2017**, *17*, 870−881; (c) Yamada, S.; Azuma, Y.; Aya, K. [2+2] Photodimerization of 1-Aryl-4-Pyridylbutadienes through Cation–π Interactions. *Tetrahedron Lett*. **2014**, *55*, 2801–2804; (d) Garai, M.; Biradha, K. One-Dimensional Coordination Polymers of Bis(3-pyridylacrylamido)ethane: Influence of Anions and Metal Ions on Their Solid State [2+2] Photochemical Polymerization and Dimerization Reactions. *Cryst*. *Growth Des*. **2017**, *17*, 925–932.

[9] (a) Claassens, I. E.; Barbour, L. J.; Haynes, D. A. A Multistimulus Responsive Porous Coordination Polymer: Temperature-Mediated Control of Solid-State [2+2] Cycloaddition. *J*. *Am*. *Chem*. *Soc*. **2019**, *141*, 11425−11429; (b) Wang, M.-F.; Mi, Y.; Hu, F.-L.; Niu, Z.; Yin, X.-H.; Huang, Q.; Wang, H.-F.; Lang, J.-P. Coordination-Driven Stereospecific Control Strategy for Pure Cycloisomers in Solid-State Diene Photocycloaddition. *J*. *Am*. *Chem*. *Soc*. **2020**, *142*, 700−704.

[10] Gan, M.-M.; Liu, J.-Q.; Zhang, L.; Wang, Y.-Y.; Hahn, F. E.; Han, Y.-F. Preparation and Post-Assembly Modification of Metallosupramolecular Assemblies from Poly(N-heterocyclic carbene) Ligands. *Chem*. *Rev*. **2018**, *118*, 9587−9641.

[11] (a) Sun, L.-Y.; Sinha, N.; Yan, T.; Wang, Y.-S.; Tan, T. T. Y.; Yu, L.; Han, Y.-F.; Hahn, F. E. Template Synthesis of Three-Dimensional Hexakisimidazolium Cages. *Angew*. *Chem*. *Int*. *Ed*. **2018**, *57*, 5161–5165; (b) Ma, L.-L.; An, Y.-Y.; Sun, L.-Y.; Wang, Y.-Y.; Hahn, F. E.; Han, Y.-F. Supramolecular Control of Photocycloadditions in Solution: In Situ Stereoselective Synthesis and Release of Cyclobutanes. *Angew*. *Chem*. *Int*. *Ed*. **2019**, *58*, 3986–3991; (c) Zhang, L.; Das, R.; Li, C.-T.; Wang, Y.-Y.; Hahn, F. E.; Hua, K.; Sun, L.-Y.; Han, Y.-F. C_3-Symmetric Assemblies from Trigonal Polycarbene Ligands and M^I Ions for the Synthesis of Three-Dimensional Polyimidazolium Cations. *Angew*. *Chem*. *Int*. *Ed*. **2019**, *58*, 13360–13364; (d) Li, Y.; Jin, G.-F.; An, Y.-Y.; Das, R.; Han, Y.-F. Metal-Carbene-Templated Photochemistry in

Solution: A Universal Route towards Cyclobutane Derivatives. *Chin*. *J*. *Chem*. **2019**, *37*, 1147–1152.

[12] (a) Yoon, J.; Kim, S. K.; Singh, N. J.; Kim, K. S. Imidazolium Receptors for the Recognition of Anions. *Chem*. *Soc*. *Rev*. **2006**, *35*, 355–360; (b) Hargrove, A. E.; Nieto, S.; Zhang, T.; Sessler, J. L.; Anslyn, E. V. Artificial Receptors for the Recognition of Phosphorylated Molecules. *Chem*. *Rev*. **2011**, *111*, 6603–6782; (c) Chen, L.-J.; Ren, Y.-Y.; Wu, N.-W.; Sun, B.; Ma, J.-Q.; Zhang, L.; Tan, H.; Liu, M.; Li, X.; Yang, H.-B. Hierarchical Self-Assembly of Discrete Organoplatinum(II) Metallacycles with Polysaccharide via Electrostatic Interactions and Their Application for Heparin Detection. *J. Am*. *Chem*. *Soc*. **2015**, *137*, 11725−11735; (d) Zhu, J.; Liu, X.; Huang, J.; Xu, L. Our Expedition in the Construction of Fluorescent Supramolecular Metallacycles. *Chin*. *Chem*. *Lett*. **2019**, *30*, 1767−1774.

[13] (a) Kim, S. K.; Sessler, J. L. Ion Pair Receptors. *Chem*. *Soc*. *Rev*. **2010**, *39*, 3784–3809; (b) Kim, D. S.; Sessler, J. L. Calix[4]pyrroles: Versatile Molecular Containers with Ion Transport, Recognition, and Molecular Switching Functions. *Chem*. *Soc*. *Rev*. **2015**, *44*, 532–546.

[14] (a) Lee, M. H.; Kim, J. S.; Sessler, J. L. Small Molecule-Based Ratiometric Fluorescence Probes for Cations, Anions, and Biomolecules. *Chem*. *Soc*. *Rev*. **2015**, *44*, 4185–4191; (b) Shirinfar, B.; Ahmed, N.; Park, Y. S.; Cho, G.-S.; Youn, S.; Han, J.-K.; Nam, H. G.; Kim, K. S. Selective Fluorescent Detection of RNA in Living Cells by using Imidazolium-Based Cyclophane. *J. Am*. *Chem*. *Soc*. **2013**, *135*, 90−93.

[15] (a) Baumgarten, M.; Yüksel, T. Synthesis and Optical Properties of Novel Blue Fuorescent Conjugated Polymers. *Phys*. *Chem*. *Chem*. *Phys*. **1999**, *1*, 1699–1706; (b) Davis, M. C.; Groshens, T. J. Synthesis of *p*-Quinquephenyl from *E*,*E*-1,4-Bis(4-bromophenyl)-1,3-butadiene. *Synth*. *Commun*. **2011**, *41*, 206–218.

[16] Huang, C.-B.; Xu, L.; Zhu, J.-L.; Wang, Y.-X.; Sun, B.; Li, X.; Yang, H.-B. Real-Time Monitoring the Dynamics of Coordination-Driven Self-Assembly by Fluorescence-Resonance Energy Transfer. *J. Am*. *Chem*. *Soc*. **2017**, *139*, 9459−9462.

(The following will be filled in by the editorial staff)
Manuscript received: XXXX, 2019
Manuscript revised: XXXX, 2019
Manuscript accepted: XXXX, 2019
Accepted manuscript online: XXXX, 2019
Version of record online: XXXX, 2019

Page No.

Formation of Functional Cyclooctadiene Derivatives by Supramolecularly-Controlled Topochemical Reactions and Their Use as Highly Selective Fluorescent Biomolecule Probes

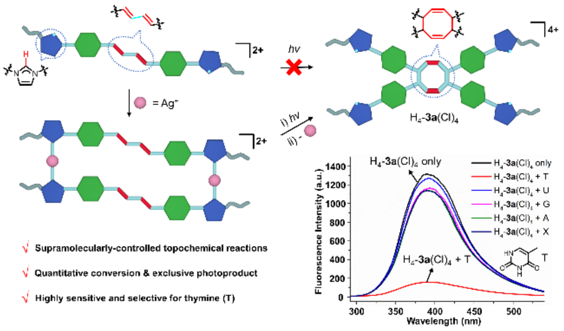

Ming-Ming Gan, and Ying-Feng Han*

A supramolecularly-controlled topochemical reaction in solution provides two cyclooctadiene-cored tetraimidazolium receptors, which exhibit highly sensitive and selective fluorescence sensing for thymine relative to other relevant molecules in aqueous solution at physiological pH (7.4).